Landsc Ecol
https://doi.org/10.1007/s10980-023-01705-y

RESEARCH ARTICLE

# Interpreting image texture metrics applied to landscape gradient data

**Kurt Riitters · Jennifer K. Costanza · John W. Coulston · Peter Vogt · Karen Schleeweis**

Received: 22 April 2023 / Accepted: 5 June 2023


**Abstract**
*Context* Pattern metrics drawn from image processing and remote sensing have been applied as descriptors of the texture of landscape gradient data. Like some classical pattern metrics in ecology, texture has several facets which are measured by examining an adjacency matrix—the frequencies of co-occurring pixel values on a map—in different ways.
*Objectives* To improve the interpretation and application of such metrics in landscape ecology we reformulate and interpret several of them by analogy to traditional metrics used with categorical data.
*Results and conclusions* 1. Four of the eight classical texture metrics measure attraction—the tendency for the same or similar values to be adjacent. Four others measure dispersion—the diversity of adjacencies relative to the entire adjacency matrix, the diagonal of the matrix, or the origin of the matrix. 2. The attraction metrics (*dissimilarity*, *contrast*, *inverse difference*, and *homogeneity*) differ only in the algebraic weights applied to different parts of an adjacency matrix. 3. The dispersion metrics (*entropy*, *uniformity*, *difference entropy*, and *sum entropy*) can be made more comparable by rescaling them to their maximum possible values. 4. While the metrics may be applied to any adjacency matrix, the choices about the method used to create an adjacency matrix have subtle yet important implications for the use and comparability of some metrics.

**Keywords** Landscape pattern · Texture metrics · Landscape gradient · Grayscale data

## Introduction

Landscape ecologists employ two general conceptual models to guide the development and application of pattern metrics in real-world problems. When a landscape is viewed as a patchwork (or network) of discrete objects such as habitat patches, the conceptual model is often referred to as the patch mosaic or the patch-corridor-matrix model (Forman and Godron 1986; Forman 1995). When a landscape is viewed as a blending of variegated habitat patches (McIntyre and Barrett 1992; McIntyre and Hobbs 1999) or as a spatially continuous habitat surface (Gustafson 1998), the conceptual model has become known as the landscape gradient model (McGarigal and Cushman 2005). Gustafson (1998) linked these concepts to the data model for different types of pattern metrics—the patch mosaic metrics typically used categorical maps

K. Riitters (✉) · J. K. Costanza · J. W. Coulston
USDA Forest Service, Southern Research Station, Asheville, USA
e-mail: kurt.h.riitters@usda.gov

P. Vogt
European Commission, Joint Research Centre, Ispra, Italy

K. Schleeweis
USDA Forest Service, Rocky Mountain Research Station, Fort Collins, USA

Published online: 22 June 2023

as a complete census of a landscape and focused on the pattern of the discrete patches, while landscape gradient metrics were derived from a sample of numeric values from discrete locations within a landscape and focused on point-data or geostatistical analysis of overall spatial pattern.

The advent of census maps portraying numeric data such as greenness, probability, and percent vegetation cover presented a new data model, potentially amenable to pattern analyses using both conceptual models (Hoechstetter et al. 2008). This has stimulated exploration of new landscape gradient pattern metrics, especially those derived from surface metrology (e.g., Hoechstetter et al. 2008; McGarigal and Cushman 2009; Abdel Moniem and Holland 2013; Kedron et al. 2018) and image analysis (e.g., St-Louis et al. 2006, 2009; Tuttle et al. 2006; Wood et al. 2013; Tuanmu and Jetz 2015). Many of the classical texture metrics from image analysis (Haralick et al. 1973) have been applied for a long time in remote sensing of natural resources (e.g., Peddle and Franklin 1991; Franklin et al. 2000; Coburn and Roberts 2004) and were first introduced as landscape pattern metrics by Musick and Grover (1991) and in landscape ecology software by Baker and Cai (1992).

While conceptual models may help to interpret landscape pattern metric values in a specific situation, they may also be limiting in the sense that pattern analysis is generic, and a metric value is just a number (Vogt and Riitters 2017). In other words, pattern is a property of a landscape and does not *require* an ecological motivation or interpretation. What *is* required is an understanding of what is measured by a pattern metric, because that is prerequisite to reliable ecological interpretation of a hypothesized pattern-process relationship (Bogaert 2003). When pattern per se is interpreted incorrectly, a pattern metric does not measure what we think it measures, and our ecological understanding is at best approximate. Later we will use the common misinterpretation of the classical contagion metric (O'Neill et al. 1988; Li and Reynolds 1993) to motivate a better understanding of what some pattern metrics measure.

Seeking an understanding of what is measured by landscape gradient metrics, some authors have turned to empirical correlations with patch mosaic metrics (e.g., McGarigal and Cushman 2009; Kedron et al. 2018). While informative, those comparisons are contingent on the underlying comparability of two different maps—the categorical map used for patch mosaic metrics and the numeric map used for landscape gradient metrics. In this paper we use another approach with only one numeric map to improve the understanding of what is measured by the texture metrics most known as *dissimilarity*, *contrast*, *inverse difference*, *homogeneity*, *entropy*, *uniformity*, *difference entropy*, and *sum entropy*. Through algebra and argument by analogy we generalize what landscape ecologists already know from experience with analogous patch mosaic metrics and show how some texture metrics may be improved by incorporating insights from the ecological literature [e.g., by rescaling entropy to a maximum value (Pielou 1966)]. While texture metrics are a small subset of the methods available to analyze landscape gradient maps, they are an important subset because texture is widely recognized as a fundamental descriptor of landscape pattern (Riitters 2019). We do not intend to recommend metrics for any specific application, but instead to provide generic metric definitions which are applicable to a wide range of applications and a framework to interpret the results in ecologically familiar terms.

Haralick (1973) texture metrics describe pixel adjacencies, also known as co-occurrences, on quantized (binned) numeric maps. The pixel adjacencies on a raster map are summarized in an adjacency matrix, also known as a co-occurrence matrix. Within an adjacency matrix, the rows and columns indicate the pixel values that are adjacent, and the elements of the matrix indicate the frequencies of each type of adjacency (Fig. 1). Texture metrics are computed from proportions calculated as the frequency of each element divided by the total frequency in the matrix (Fig. 1). This is the same data reduction process used to calculate the well-known contagion metric from nominal data (O'Neill et al. 1988; Li and Reynolds 1993).

The key to improving the ecological interpretation of texture metrics applied to numeric data is to notice that quantized numeric maps portray ordinal data, which are categorical data where the numeric value of a pixel is meaningful. Thus, it is reasonable to expect that insights gained from ecological applications of well-known metrics with dichotomous or nominal data may improve the interpretation of texture metrics with real-valued data. Furthermore, many of the available numeric maps are quantized for efficient storage or analysis anyway. From a metric computation

Input map with four pixel values, 25 pixels, and 40 adjacencies

| | | | | |
|---|---|---|---|---|
| 0 | 3 | 3 | 0 | 1 |
| 0 | 1 | 0 | 1 | 0 |
| 1 | 1 | 0 | 2 | 0 |
| 0 | 0 | 0 | 0 | 0 |
| 0 | 0 | 1 | 1 | 1 |

Adjacency matrices (ordered)

Frequency $x(i,j)$

| | 0 | 1 | 2 | 3 |
|---|---|---|---|---|
| 0 | 12 | 9 | 1 | 1 |
| 1 | 6 | 4 | 1 | 0 |
| 2 | 2 | 0 | 0 | 0 |
| 3 | 2 | 1 | 0 | 1 |

Proportion $p(i,j)$

| | 0 | 1 | 2 | 3 |
|---|---|---|---|---|
| 0 | 0.300 | 0.225 | 0.025 | 0.025 |
| 1 | 0.150 | 0.100 | 0.025 | 0 |
| 2 | 0.050 | 0 | 0 | 0 |
| 3 | 0.050 | 0.025 | 0 | 0.025 |

Adjacency matrices (unordered)

Frequency $x'(i,j)$

| | 0 | 1 | 2 | 3 |
|---|---|---|---|---|
| 0 | 12 | 15 | 3 | 3 |
| 1 | - | 4 | 1 | 1 |
| 2 | - | - | 0 | 0 |
| 3 | - | - | - | 1 |

Proportion $p'(i,j)$

| | 0 | 1 | 2 | 3 |
|---|---|---|---|---|
| 0 | 0.300 | 0.375 | 0.075 | 0.075 |
| 1 | - | 0.100 | 0.025 | 0.025 |
| 2 | - | - | 0 | 0 |
| 3 | - | - | - | 0.025 |

**Fig. 1** Illustration of the ordered and unordered adjacency matrices for a 2-neighbor rule defined as "one pixel below or one pixel to the right." The pixel values labeled as 0, 1, 2, 3 may represent nominal or ordinal values. Adjacency frequencies and proportions are calculated as defined in Table 1. Adjacencies at the map border are ignored. The total number of adjacencies is 40, and the numbers of unique adjacencies in the ordered and unordered matrices are 16 and 10, respectively

perspective, the only difference between dichotomous, nominal, and ordinal maps is that in the latter, the numeric differences between pixel values are meaningful. Our primary objectives here are to summarize an understanding of what eight commonly used texture metrics measure on quantized numeric maps, and to suggest how those metrics can be extended or improved by using insights gained from previous ecological treatments of categorical maps. We also reformulate defining equations to facilitate metric comparisons, and address computational issues.

## Methods

### Preliminary considerations

In principle, metric computation is independent of the data reduction procedure used to create an adjacency matrix. However, it is necessary to understand the reduction procedure to understand the metric. For example, the well-known 4-neighbor procedure examines the adjacency of a given pixel with respect to the four neighboring pixels in cardinal directions. Since the procedure is also applied to all four neighboring pixels, this procedure counts each adjacency twice (i.e., as both [pixel 1, pixel 2] and [pixel 2, pixel 1]). In other words, 4-neighbor procedure yields a symmetric adjacency matrix. This becomes important for metrics such as entropy because it violates an assumption that each element in the adjacency matrix represents a unique state. For that reason, our data reduction procedure uses a 2-neighbor procedure by which each adjacency is counted once, tabulating the pair [pixel 1, pixel 2] separately from the pair [pixel 2, pixel 1], yielding an ordered adjacency matrix (Fig. 1). Since pixel order is arguably arbitrary (e.g., inverting the input map would transpose the adjacency matrix), it can be removed to construct an unordered adjacency matrix (Fig. 1). Where appropriate we provide metric definitions for both the ordered and unordered cases which do not violate the assumptions of the metrics.

Metric definitions must also consider the extent of the map which is used to create an adjacency matrix. For example, in a global analysis the entire map extent is used, whereas in a moving window analysis the extent is defined by a window which contains a portion of the map. Because the purpose of a moving window analysis is to localize the metric calculation to create a map of a given metric, the calculated metric must be comparable for all windows across the global extent. For example, some metrics are rescaled to maximum values which depend on the number of unique states in an adjacency matrix, which cannot be assumed to be constant for all windows. Our metric definitions are structured for applications to both global and window extents.

The assumptions regarding the characteristics of the input data are especially important when comparing metric definitions in the literature. Specifically, it is important to know whether the range of pixel values includes or excludes both negative and zero values. For example, the original Haralick (1973) metrics exclude negative and zero values, which required rescaling the input data to apply the metrics to a map of a vegetation index (Tuanmu and Jetz 2015). However, for some types of maps (e.g., a map of percent vegetation cover) a zero value is meaningful. Accommodating these nuances required minor modification of some published metric definitions. We assume that input data has been appropriately rescaled and quantized to ordinal integers in [0, 1, 2, 3…]. It is recognized that different types of quantization may affect the realized metric values (e.g., Löfstedt et al. 2019), but sensitivity to quantization is beyond the scope of this paper. We use the notation in Table 1 when later defining metrics.

## Interpreting metrics

### Attraction metrics

The classical landscape metric of clumping (called contagion by O'Neill et al. 1988) was motivated to detect the tendency for each pixel category to appear in contiguous patches of the same category. Like the well-known Shannon index of species evenness (Pielou 1966), it is a rescaled measure of entropy that accounts for the number of unique states (here, the states are defined by the types of adjacencies instead of the types of species). The metric usually works as a patch mosaic metric because dichotomous and nominal maps typically exhibit contiguous patches of the same pixel value, such that there is an over-abundance of observations in the diagonal elements of an adjacency matrix, which reduces entropy. However,

**Table 1** Notation used for metric definitions

| Notation | Definition | Notes |
|---|---|---|
| $i,j$ | Pixel values $i$ (row) and $j$ (column) in the adjacency matrix formed by 2-neighbor adjacencies | $i,j \in [0,1,2,3\ldots]$ |
| $x(i,j)$ | Element $i, j$ in the adjacency matrix | Ordered adjacency frequencies |
| $x^{'}(i,j)$ | $\begin{cases} x(i,j)+x(j,i), \; if\ i \neq j \\ x(i,j), \; if\ i=j \end{cases}$ | Unordered adjacency frequencies |
| $p(i,j)$ | $\frac{x(i,j)}{\sum_i \sum_j x(i,j)}$ | Ordered adjacency proportions |
| $p'(i,j)$ | $\frac{x^{'}(i,j)}{\sum_i \sum_j x(i,j)}$ | Unordered adjacency proportions |
| $p_{x-y}(k)$ | $\sum_i \sum_{j\ where\ \|i-j\|=k} p(i,j)$ | Difference function (Haralick et al. 1973) |
| $p_{x+y}(k)$ | $\sum_i \sum_{j\ where\ i+j=k} p(i,j)$ | Sum function (Haralick et al. 1973) |
| $N_g$ | Number of unique pixel values in the adjacency matrix | |
| $N_k$ | Number of $k$ levels in the adjacency matrix | |
| $k^*$ | Selected $k$ level | User-selected |
| $I_k$ | $\begin{cases} 1, if\ k \leq k^* \\ 0, if\ k > k^* \end{cases}$ | Indicator variable |

it is an unreliable measure of contagion because it is equally sensitive to an over-abundance of adjacencies that are not diagonal elements, which also reduce entropy but do not indicate contagion (Riitters et al. 1996). For this reason, Riitters et al. (1995) proposed an alternate contagion metric ($D_A$ in Table 2) which is the sum of only the diagonal elements of an adjacency matrix.

To develop interpretations of related Haralick metrics, the first step is to define the difference function ($p_{x-y}(k)$ in Table 1) which calculates the proportions of all adjacencies for which the absolute value of the difference between adjacent pixel values equals $k$ (see example in Fig. 2). With that, $D_A$ can be generalized to *k-attraction* for ordinal maps (Table 2) for which the parameter $k$ is a threshold numeric difference between two adjacent pixels. For $k=0$, only the diagonal elements of an adjacency matrix are included, and *k-attraction* is equivalent to $D_A$. For a selected value of $k>0$, an off-diagonal element of the adjacency matrix is included if the numeric difference between pixel values is less than or equal to $k$. As an alternative to contagion, the term attraction thus refers to the tendency for *the same or similar values* to be adjacent on dichotomous, nominal, and ordinal maps.

The next step is to reformulate the Haralick metrics called *dissimilarity*, *contrast*, *inverse difference*, and *homogeneity* using the same difference function that was used for *k-attraction*. It is then apparent that the Haralick metrics are weighted sums of the difference function and that the weights are a function of $k$ (Table 2). In other words, these metrics differ only by the weights applied to adjacencies at the distance ($k$) from the diagonal of the adjacency matrix. The weight is linear with respect to $k$ for the *dissimilarity* and *inverse difference* metrics and nonlinear for the *contrast* and *homogeneity* metrics. The *inverse difference* and *homogeneity* metrics include the diagonal elements of the adjacency matrix, are bounded in [0,1], and larger values indicate more attraction, while *dissimilarity* and *contrast* exclude the diagonal elements, are unbounded, and larger values indicate less attraction (or more repulsion). For *k-attraction* the weights are a [1, 0] step function of $k$; the metric includes the diagonal elements of the adjacency matrix, is bounded in [0, 1], and larger values indicate more attraction. Based on algebraic similarity alone, the realized values for all attraction metrics are expected to be correlated to some degree, as illustrated by an application to a map of percent tree cover (Fig. 3). While all these metrics are plausible choices for measuring the aspect of pattern called attraction, an understanding of their algebraic differences should help to inform the choices of a metric for a specific application.

## Dispersion metrics

The Haralick metrics called *entropy* and *uniformity* are natural extensions of well-known species diversity metrics, only as applied to describe the diversity of adjacencies instead of the diversity of species. In fact, *entropy* is the Shannon index, and *uniformity* (also known as *angular second moment* and *energy*) is the complement of the Gini-Simpson index. Without

**Table 2** Attraction metrics, illustrating the reformulation of the typical literature definition using the difference function

| Metric [reference] | Typical literature formulation | Reformulation using difference function |
|---|---|---|
| $D_A$ [1] | $\sum_i [p(i,i)]$ | $p_{x-y}(0)$ |
| $k$-attraction | Not applicable | $\sum_k \left[ I_k \cdot p_{x-y}(k) \right]$ |
| Dissimilarity [2] | $\sum_i \sum_j [\lvert i-j \rvert \cdot p(i,j)]$ | $\sum_k \left[ k \cdot p_{x-y}(k) \right]$ |
| Contrast [3, 4] | $\sum_i \sum_j [(i-j)^2 \cdot p(i,j)]$ | $\sum_k \left[ k^2 \cdot p_{x-y}(k) \right]$ |
| Inverse difference [4] | $\sum_i \sum_j \left[ \frac{p(i,j)}{1+\lvert i-j \rvert} \right]$ | $\sum_k \left[ \left( \frac{1}{1+k} \right) \cdot p_{x-y}(k) \right]$ |
| Homogeneity [2, 3] | $\sum_i \sum_j \left[ \frac{p(i,j)}{1+(i-j)^2} \right]$ | $\sum_k \left[ \left( \frac{1}{1+k^2} \right) \cdot p_{x-y}(k) \right]$ |

The reformulations of the last four metrics substitute $k = i - j$, and $\sum_k p_{x-y}(k) = \sum_i \sum_j p(i,j)$. The reference numbers in the table refer to: 1—Riitters et al. (1995); 2—Soh and Tsatsoulis (1999); 3—Haralick et al. (1973); 4—Clausi (2002) *k* values for difference function

| | 0 | 1 | 2 | 3 |
|---|---|---|---|---|
| 0 | 0 | 1 | 2 | 3 |
| 1 | 1 | 0 | 1 | 2 |
| 2 | 2 | 1 | 0 | 1 |
| 3 | 3 | 2 | 1 | 0 |

*k* values for sum function

| | 0 | 1 | 2 | 3 |
|---|---|---|---|---|
| 0 | 0 | 1 | 2 | 3 |
| 1 | 1 | 2 | 3 | 4 |
| 2 | 2 | 3 | 4 | 5 |
| 3 | 3 | 4 | 5 | 6 |

Illustration of difference function $p_{x-y}(k)$ using ordered adjacencies

| | 0 | 1 | 2 | 3 |
|---|---|---|---|---|
| 0 | 0.300 | 0.225 | 0.025 | 0.025 |
| 1 | 0.150 | 0.100 | 0.025 | 0 |
| 2 | 0.050 | 0 | 0 | 0 |
| 3 | 0.050 | 0.025 | 0 | 0.025 |

$p_{x-y}(0) = 0.3 + 0.1 + 0 + 0.025 = 0.425$

$p_{x-y}(1) = 0.225 + 0.025 + 0 + 0 + 0.15 + 0 + 0 = 0.4$

$p_{x-y}(2) = 0.025 + 0 + 0.05 + 0.025 = 0.1$

$p_{x-y}(3) = 0.025 + 0.05 = 0.075$

$$\sum_k p_{x-y}(k) = 1.0$$

Illustration of sum function $p_{x+y}(k)$ using ordered adjacencies

| | 0 | 1 | 2 | 3 |
|---|---|---|---|---|
| 0 | 0.300 | 0.225 | 0.025 | 0.025 |
| 1 | 0.150 | 0.100 | 0.025 | 0 |
| 2 | 0.050 | 0 | 0 | 0 |
| 3 | 0.050 | 0.025 | 0 | 0.025 |

$p_{x+y}(0) = 0.3$

$p_{x+y}(1) = 0.15 + 0.225 = 0.375$

$p_{x+y}(2) = 0.05 + 0.1 + 0.025 = 0.175$

$p_{x+y}(3) = 0.05 + 0 + 0.025 + 0.025 = 0.1$

$p_{x+y}(4) = 0.025 + 0 + 0 = 0.025$

$p_{x+y}(5) = 0 + 0 = 0$

$p_{x+y}(6) = 0.025$

$$\sum_k p_{x+y}(k) = 1.0$$

**Fig. 2** A worked example of the difference and sum functions for ordinal data. Step 1: the *k* values correspond to a given sum or absolute difference of the corresponding row and column labels. In the difference matrix, *k* increases with distance from the diagonal (top left). In the sum matrix, *k* increases with distance from the origin (top right). Step 2: the ordered proportions from Fig. 1 are inserted into the adjacency matrices (middle left and bottom left). Step 3: for a given value of *k*, the difference and sum functions are the sums of proportions having that *k* value (middle right and bottom right); the *k* values are color-coded for each function

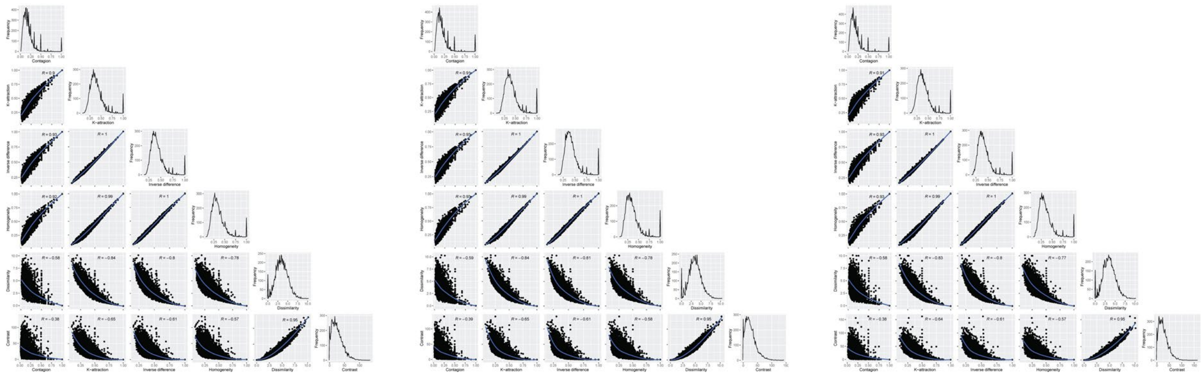

**Fig. 3** Correlation among attraction metrics from moving window analyses of a map of percent tree cover. The input map depicted tree cover percent for the conterminous United States (USGS 2019) after re-sampling to 2430 m resolution. Maps of metric values were created by moving window analyses in which input pixel values equal to zero were treated as missing data and metric values were assigned to the pixel at the center of a given window. A threshold $k = 5$ was used for the *k-attraction* metric. The 8000 points and loess curves shown in the charts are a ~ 1% random sample of the output pixels for three cases: (left) percent tree cover in [1, 100] with a 15 pixels × 15 pixels moving window; (middle) percent tree cover rescaled to [1, 20] with a 15 × 15 moving window; (right) percent cover rescaled to [1, 20] with a 7 × 7 moving window

going any further, these Haralick metrics are thus already interpretable as measures of the dispersion of observations within an adjacency matrix (analogous to the dispersion of individuals among species). The choice between them is also familiar—*entropy* is more sensitive to rare observations while *uniformity* is more sensitive to abundant observations—as is the concept of rescaling metrics to their maximum possible values to improve comparability among different sets of observations. Here we can suggest several little-used or novel variations of these Haralick metrics which include rescaling and accounting for the differences between ordered and unordered adjacencies (Table 3).

We develop rescaling procedures following the general rationale of Li and Reynolds (1993) to define maximum possible values. We start with the usual expression for *entropy* but use (Gini–Simpson) *diversity* to represent *uniformity* (Table 3). The maximum possible values for *entropy* and *diversity* depend on the potential number of unique adjacencies in an adjacency matrix. If $N$ is the number of unique pixel values (not adjacency values) in an adjacency matrix, then the number of possible adjacencies is $N^2$ when adjacencies are ordered, and $\left(N^2 + N\right)/2$ when adjacencies are unordered. When all adjacencies are equally likely, they all equal $1/N^2$ (ordered adjacencies) or $2/\left(N^2 + N\right)$ (unordered adjacencies). Solving the defining *entropy* and *diversity* equations (Table 3) for those quantities yields the maximum values for *entropy* (ordered: $2 \cdot \ln N$; unordered: $\ln\left(N^2 + N\right) - \ln 2$) and *diversity* (ordered: $1 - \left(1/N^2\right)$; unordered: $1 - \left[2/\left(N^2 + N\right)\right]$). A metric is rescaled with division by its maximum value, yielding the *evenness* and *equitability* metrics for ordered and unordered adjacencies (Table 3).

Finally, we consider Haralick's *difference entropy* and *sum entropy* metrics. They describe the overall dispersion of adjacencies relative to the diagonal (*difference entropy*) or the origin (*sum entropy*) of the adjacency matrix (Fig. 2). For these metrics the order of adjacencies is irrelevant, but like *entropy* they can be rescaled for comparability among sets of observations. For computational efficiency and to illustrate rescaling according to the realized number of unique states, we suggest the maximum value of $\ln K$, where $K$ is the number of unique $k$ values in an adjacency matrix, derived analogously to the maximum Shannon diversity index (Pielou 1966).

## Discussion

The science and practice of pattern measurement will continue to evolve, driven by new conceptual models and data sources, capitalizing on metrics developed within other fields, and informed by applications to the burgeoning data stream with ever-improving

**Table 3** Dispersion metrics

| Metric [Reference] | Definition | Notes [Reference] |
|---|---|---|
| Entropy (ordered adjacencies) [1] | $-\sum_i \sum_j [p(i,j) \cdot \ln p(i,j)],\ for\ p(i,j) > 0$ | |
| Evenness (ordered adjacencies) [2] | $\frac{Entropy}{2 \cdot \ln N_g},\ for\ N_g > 1$ | Uses ordered entropy |
| Entropy (unordered adjacencies) [3] | $-\sum_i \sum_{j \geq i} \left[p'(i,j) \cdot \ln p'(i,j)\right],\ for\ p'(i,j) > 0$ | |
| Evenness (unordered adjacencies) [3] | $\frac{Entropy}{\left[\ln\left(N_g^2 + N_g\right) - \ln 2\right]},\ for\ N_g > 1$ | Uses unordered entropy |
| Diversity (ordered adjacencies) [1, 4] | $1 - \sum_i \sum_j [p(i,j) \cdot p(i,j)]$ | Complement of uniformity [5] |
| Equitability (ordered adjacencies) [4] | $\frac{Diversity}{1 - \left(1/N_g^2\right)},\ for\ N_g > 1$ | Uses ordered diversity |
| Diversity (unordered adjacencies) | $1 - \sum_i \sum_{j \geq i} \left[p'(i,j) \cdot p'(i,j)\right]$ | |
| Equitability (unordered adjacencies) | $\frac{Diversity}{1 - \left[2/\left(N_g^2 + N_g\right)\right]},\ for\ N_g > 1$ | Uses unordered diversity |
| Difference entropy [1] | $-\sum_k [p_{x-y}(k) \cdot \ln p_{x-y}(k)]$ | |
| Difference evenness | $\frac{Difference\ entropy}{\ln N_k},\ for\ N_k > 1$ | |
| Sum entropy [1] | $-\sum_k [p_{x+y}(k) \cdot \ln p_{x+y}(k)]$ | |
| Sum evenness | $\frac{Sum\ entropy}{\ln N_k},\ for\ N_k > 1$ | |

The reference numbers in the first column refer to: 1—Haralick et al. (1973); 2—Li and Reynolds (1993); 3—Riitters et al. (1996); 4—Wickham and Riitters (1995); 5—Clausi (2002)

computing capacity (Costanza et al. 2019). The texture metrics described here were derived largely within the field of image processing; while they have been used extensively in remote sensing and medical imaging there are fewer applications in landscape ecology. In the past, the introduction of a new landscape pattern metric has typically required a demonstration that it was different or better in some way from those already available, but rarely has a new metric been gauged against a standard of understanding what it measures. With a new understanding of what is measured by texture metrics on numeric maps, we can more clearly see the relationships between them, and to the landscape ecology metrics which have been applied to categorical maps, and we can use insights gained from the latter to improve and interpret the texture metrics in an ecological context.

We can suggest two plausible lines for future research. First, it is well-known in the ecology literature that the classical entropy and diversity metrics are sensitive to the total number of species. Similarly, an unequal abundance of pixel values affects the entropy and diversity of adjacencies because the more abundant pixel values naturally have a higher frequency of adjacencies than the rare pixel values. That is the rationale for using what are known as conditional metrics (e.g., Li and Reynolds 1993; Nowosad and Stepinski 2019), for which the proportions in an adjacency matrix are based on the frequency of adjacencies involving a given pixel value instead of the total frequency of all adjacencies. Li and Reynolds (1993) provided an appropriate rescaling of *entropy* for that case, and rescaling could be developed analogously for *diversity*. Future research to develop other related metrics (e.g., Nowosad and Stepinski 2019) may also be considered. Second, while the Haralick metrics which are based on numerical differences between adjacent pixels have no computational equivalent for dichotomous or nominal maps, we have shown that metrics for the latter are useful for informing the interpretation of the former. Future work could explore alternate definitions of additional Haralick metrics so that the same definition can apply to all three types of categorical data. In this regard, we can suggest that the similarity indices proposed by Gower (1971) for all three types of categorical data could help to bridge the gap. Gower (1971) also suggested rescaling alternatives which could improve the comparability of the attraction metrics among sets of observations.

**Acknowledgements** This work was performed in the context of a research agreement between the USDA Forest Service (Memorandum of Understanding #14-MU-11330110-001) and the European Commission Joint Research Centre (Collaborative Research Arrangement #33385).

**Author contributions** All authors contributed to the study conception and design. The first draft of the manuscript was written by KR and all authors commented on previous versions of the manuscript. All authors read and approved the final manuscript.

**Funding** The authors declare that no funds, grants, or other support were received during the preparation of this manuscript.

**Data availability** Data used to prepare Fig. 3 are available from the corresponding author on request.

**Declarations**

**Competing interests** The authors have no relevant financial or non-financial interests to disclose.

## References

Abdel Moniem HEM, Holland JD (2013) Habitat connectivity for pollinator beetles using surface metrics. Landsc Ecol 28:1251–1267

Baker WL, Cai Y (1992) The r.le programs for multiscale analysis of landscape structure using the GRASS geographical information system. Landsc Ecol 7:291–302

Bogaert J (2003) Lack of agreement on fragmentation metrics blurs correspondence between fragmentation experiments and predicted effects. Ecol Soc 7(1):r6

Clausi DA (2002) An analysis of co-occurrence texture statistics as a function of grey level quantization. Can J Remote Sens 28:45–62

Coburn CA, Roberts AC (2004) A multiscale texture analysis procedure for improved forest stand classification. Int J Remote Sens 25:4287–4308

Costanza JK, Riitters K, Vogt P, Wickham J (2019) Describing and analyzing landscape patterns: where are we now, and where are we going? Landsc Ecol 34:2049–2055

Forman RTT (1995) Land mosaics: the ecology of landscapes and regions. Cambridge University Press, Cambridge

Forman RTT, Godron M (1986) Landscape ecology. Wiley, New York

Franklin SE, Hall RJ, Moskal LM, Maudie AJ, Lavigne MB (2000) Incorporating texture into classification of forest species composition from airborne multispectral images. Int J Remote Sens 21:61–79

Gower JC (1971) A general coefficient of similarity and some of its properties. Biometrics 27:857–871

Gustafson E (1998) Quantifying landscape spatial pattern: what is the state of the art? Ecosystems 1:143–156

Haralick RM, Shanmugam K, Dinstein I (1973) Textural features for image classification. IEEE Trans Syst Man Cybern 3(6):610–621

Hoechstetter S, Walz U, Dang LH, Thinh NX (2008) Effects of topography and surface roughness in analyses of landscape structure—a proposal to modify the existing set of landscape metrics. Landsc Online 3:1–14

Kedron PJ, Frazier AE, Ovando-Montejo GA, Wang J (2018) Surface metrics for landscape ecology: a comparison of landscape models across ecoregions and scales. Landsc Ecol 33:1489–1504

Li H, Reynolds JF (1993) A new contagion index to quantify spatial patterns of landscapes. Landsc Ecol 8:155–162

Löfstedt T, Brynolfsson P, Asklund T, Nyholm T, Garpebring A (2019) Gray-level invariant Haralick texture features. PLoS ONE 14(2):e0212110

McGarigal K, Cushman SA (2005) The gradient concept of landscape structure. In: Wiens J, Moss M (eds) Issues and perspectives in landscape ecology. Cambridge University Press, Cambridge, pp 112–119

McGarigal K, Tagil S, Cushman SA (2009) Surface metrics: an alternative to patch metrics for the quantification of landscape structure. Landsc Ecol 24:433–450

McIntyre S, Barrett GW (1992) Habitat variegation, an alternative to fragmentation. Conserv Biol 6:146–147

McIntyre S, Hobbs R (1999) A framework for conceptualizing human effects on landscapes and its relevance to management and research models. Conserv Biol 13:1282–1292

Musick HB, Grover HD (1991) Image textural measures as indices of landscape pattern. In: Turner MJ, Gardner RH (eds) Quantitative methods in landscape ecology. Springer-Verlag, New York, pp 77–104

Nowosad J, Stepinski TF (2019) Information theory as a consistent framework for quantification and classification of landscape patterns. Landsc Ecol 34:2091–2101

O'Neill RV, Krummel JR, Gardner RH, Sugihara G, Jackson B, DeAngelis DL, Milne BT, Turner MG, Zygmunt B, Christensen SW, Dale VH, Graham RL (1988) Indices of landscape pattern. Landsc Ecol 1:153–162

Peddle D, Franklin S (1991) Image texture processing and data integration for surface pattern discrimination. Photogramm Eng Remote Sens 57:413–420

Pielou EC (1966) The measurement of diversity in different types of biological collections. J Theor Biol 13:131–144

Riitters K (2019) Pattern metrics for a transdisciplinary landscape ecology. Landsc Ecol 34:2057–2063

Riitters KH, O'Neill RV, Hunsaker CT, Wickham JD, Yankee DH, Timmins SP, Jones KB, Jackson BL (1995) A factor analysis of landscape pattern and structure metrics. Landsc Ecol 10:23–39

Riitters KH, O'Neill RV, Wickham JD, Jones KB (1996) A note on contagion indices for landscape analysis. Landsc Ecol 11:197–202

Soh L-K, Tsatsoulis C (1999) Texture analysis of SAR sea ice imagery using gray level co-occurrence matrices. IEEE Trans Geosci Remote Sens 37:780–795

St-Louis V, Pidgeon AM, Radeloff VC, Clayton MK (2006) High-resolution image texture as a predictor of bird species richness. Remote Sens Environ 105:299–312

St-Louis V, Pidgeon AM, Clayton MK, Locke BA, Bash DW, Radeloff VC (2009) Satellite image texture and a

vegetation index predict avian biodiversity in the Chihuahuan Desert of New Mexico. Ecography 32:468–480
Tuanmu M-N, Jetz W (2015) Global habitat heterogeneity. Glob Ecol Biogeogr 24:1329–1339
Tuttle EM, Jensen RR, Formica VA, Gonser RA (2006) Using remote sensing image texture to study habitat use patterns: a case study using the polymorphic white-throated sparrow (*Zonotrichia albicollis*). Glob Ecol Biogeogr 15:349–357
USGS (United States Geological Survey) (2019) NLCD 2016 tree canopy cover (CONUS). U.S. Geological Survey, Sioux Falls, SD. https://www.mrlc.gov/data/nlcd-2016-usfs-tree-canopy-cover-conus
Vogt P, Riitters K (2017) GuidosToolbox: universal digital image object analysis. Eur J Remote Sens 50:352–361
Wickham JD, Riitters KH (1995) Sensitivity of landscape metrics to pixel size. Int J Remote Sens 16:3585–3594
Wood EM, Pidgeon AM, Radeloff VC, Keuler NS (2013) Image texture predicts avian density and species richness. PLoS ONE 8(5):e63211